Inverse Problems 10 (1994) 1345–1360 Printed in the UK

Analysis of the discrete Beck method of solving ill-posed parabolic equations

Hans-Jürgen Reinhardt
Universität GH Siegen, FB Mathematik and FOMAAS, 57068 Siegen, Germany

Received 8 January 1993, in final form 2 November 1993

Abstract. A matrix formulation of the Beck method of solving the inverse heat conduction problem is developed. A classical approach using maximum principles is applied, in order to obtain stability estimates for the sequential procedure approximating the surface heat fluxes. On the basis of our estimates, a stronger form of the classical Courant–Friedrichs–Lewy condition ensures stability in a certain weak sense. Finally, numerical results are presented and discussed in view of the stability condition.

1. Introduction

In a series of engineering problems concerning heat transfer processes, it is required to calculate the transfer surface heat flux and the surface temperature from a temperature history measured at fixed locations inside the body or on other parts of the surface. These problems are well known under the name inverse heat conduction problems (IHCP); references can be found in [4, 9, 16] and references therein.

The problem described above belongs to a class of ill-posed boundary value problems for parabolic equations that are known to be severely ill posed. The formulation of such problems leads to a non-characteristic Cauchy problem for parabolic equations. In this paper the heat equation in its simplest form is studied as a model problem.

For such problems, stability estimates of the Hölder type are established (see, for example, [5, 8, 11–14, 19]. The estimates of Carasso [5] are interesting in the sense that they are not only in L_2-norm but also in L_∞-norm. In contrast to [5, 13, 14, 19], where the problems are considered on infinite or on semi-infinite intervals with constant coefficients, the works of [8, 10, 11] treat finite time intervals with variable coefficients. Numerical approximations are also considered in some of these papers, but no estimates for the discretizations are provided.

There are several approximating procedures available among which we concentrate on sequential ones stepping forward in time. Among these the method of Beck [2, 3] is well established and has been successfully used for about thirty years. It is interesting, however, that even in the simplest one-dimensional setting for the Beck method there is no theoretical basis for the choice of the two essential parameters, i.e. the size of the time steps, Δt, and the number, r, of future times. A first attempt in this direction is made in [18].

For the Beck method studied in this paper, no Hölder-type estimates are known, nor can be provided here. Instead of estimating the error between the solutions of the non-characteristic Cauchy problem and the Beck method, only the stability behaviour of the sequential procedure itself is analysed. More specifically, in this paper, the discrete version of the Beck method is studied and, from the viewpoint of the classical stability analysis of time stepping algorithms, the growth of the (theoretical) bounds is analysed. The estimates are not of Hölder type but contain computable quantities (see $S_\Delta^{(r)}$ in (19), (20) and (23)), which reflect the ill-posed character of the problem.

In this paper we develop a matrix formulation for the Beck method of solving the one-dimensional IHCP. As representatives, the well known backward Euler and Crank–Nicolson difference methods are considered. The aim of this paper is to demonstrate how a classical approach, used for discretization methods solving initial value problems, can be applied to obtain stability estimates for the sequential procedure approximating the heat fluxes and the corresponding solutions of the ill-posed heat equation. Here, an approach using positivity properties and maximum principles is applied. Other techniques, e.g. discrete Fourier analysis, may be utilized in a similar way.

In section 2, a matrix formulation of the one-dimensional heat equation is given. Using this as a basis, in section 3 the Beck method for solving the IHCP is written down in discrete form. As a result, the desired surface fluxes and temperatures satisfy a system of equations which has a similar form to those for discretization methods for initial value problems. According to the ill-posed character of the problem, a certain extension of the classical approach is present here. Using the classical point of view, we are able to obtain stability estimates in section 4 showing how the surface heat fluxes at time t_{n+1} can be bounded by corresponding quantities at the previous time t_n. On the basis of our estimates, a stability condition is formulated in a way which can be understood as a stronger form of the well known Courant–Friedrichs–Lewy condition (see (23)). It requires a boundedness of the mesh ratio $\Delta t/h$. In section 5 computational results for three examples of IHCPs are presented for various Δt and r. The numerical results are discussed in view of our stability condition.

2. Problem setting and discretization methods

The linear inverse heat conduction problem in one spatial dimension in its simplest form can be formulated as follows:

The one-dimensional linear inverse heat conduction problem. For a given data function $g(t)$ and an initial temperature distribution u_0, find $f(t) = u(0,t)$ and $q(t) = -u_x(0,t)$, $0 < t \leqslant T$, such that

$$\begin{array}{lll} u_t - u_{xx} = 0 & & 0 < x < 1,\ 0 < t \leqslant T \\ u_x(1,t) = 0 & u(1,t) = g(t) & 0 < t \leqslant T \\ u(x,0) = u_0(x) & & 0 < x < 1. \end{array} \tag{1}$$

To obtain approximate solutions, we discretize the spatial interval using J, not necessarily equidistant, subintervals and subdivide the time interval in equidistant time steps of size Δt denoting $t_n = n\Delta t$, $n = 0, \ldots, N$. Then the (direct) heat equation with flux boundary conditions at both ends of the spatial interval in a discretized form reads

$$C_\Delta^{(0)} u^{n+1} - \Delta t\big(Q_0^{(0)} q_0^{n+1} + Q_J^{(0)} q_J^{n+1}\big) = C_\Delta^{(1)} u^n + \Delta t\big(Q_0^{(1)} q_0^n + Q_J^{(1)} q_J^n\big)$$
$$n = 0, \ldots, N-1. \tag{2}$$

Here, $C_\Delta^{(i)}$, $i = 0, 1$, are $(J+1) \times (J+1)$ matrices, $C_\Delta^{(0)}$ is assumed to be non-singular, $Q_\nu^{(i)}$ are linear operators mapping a number ϕ to the $(J+1)$-vector with a multiple of ϕ in the νth component and zero otherwise, and q_0^μ, q_J^μ are approximations of the heat fluxes at $x = 0$ and $x = 1$, respectively, at time t_μ, $\mu = n, n+1$.

The mappings $Q_\nu^{(i)}$ can be expressed by $(J+1)$-vectors

$$Q_\nu^{(i)} = (0, \ldots, 0, \alpha^{(i)}, 0, \ldots, 0)^{\mathrm{T}} \qquad \nu \in \{0, \ldots, J\},\ i = 0, 1.$$

For example, if we use the *backward Euler (BE) method* in time, with the central difference quotient for approximating u_{xx} on equidistant spatial intervals of length h, we obtain (see, e.g. 4.1.(10) in [15])

$$C_\Delta^{(0)} = A - \Delta t B \qquad C_\Delta^{(1)} = A \tag{3}$$

$$Q_0^{(0)} = \frac{2}{h}(1, 0, \ldots, 0)^{\mathrm{T}} \qquad Q_J^{(0)} = \frac{2}{h}(0, \ldots, 0, 1)^{\mathrm{T}} \qquad Q_0^{(1)} = Q_J^{(1)} = (0, \ldots, 0)^{\mathrm{T}} \tag{4}$$

with $A = E$ and

$$B = \frac{1}{h^2}\begin{pmatrix} -2 & 2 & 0 & & & & 0 \\ 1 & -2 & 1 & 0 & & & \\ 0 & 1 & -2 & 1 & 0 & & \\ & & & \ddots & & & \\ & & & & \ddots & & \\ & & & 0 & 1 & -2 & 1 \\ 0 & & & & 0 & 2 & -2 \end{pmatrix}.$$

The well known *Crank–Nicolson (CN) method* also using the central difference quotient for the spatial derivative leads to

$$C_\Delta^{(0)} = A - \frac{\Delta t}{2}B \qquad C_\Delta^{(1)} = A + \frac{\Delta t}{2}B \tag{5}$$

$$\begin{aligned} Q_0^{(0)} &= \frac{1}{h}(1, 0, \ldots, 0)^{\mathrm{T}} \qquad Q_J^{(0)} = \frac{1}{h}(0, \ldots, 0, 1)^{\mathrm{T}} \\ Q_0^{(1)} &= \frac{1}{h}(1, 0, \ldots, 0)^{\mathrm{T}} \qquad Q_J^{(1)} = \frac{1}{h}(0, \ldots, 0, 1)^{\mathrm{T}} \end{aligned} \tag{6}$$

with A and B as in (3).

The standard Galerkin methods, e.g. with continuous piecewise linear basis functions, can be written in the same way (2) where the matrices have to be defined appropriately (see, e.g. 4.2.(22) in [15]).

Properties of the matrices A and B are well known. For example, $-B$ in (3) is a positive definite M-matrix. By positivity arguments, or by studying the amplification factors of the above methods, one can ensure the invertibility of $C_\Delta^{(0)}$ and the uniform boundedness of arbitrary powers of $C_\Delta = C_\Delta^{(0)-1} C_\Delta^{(1)}$ (cf 12.1 and 12.2 in [15]).

3. The Beck method in discrete form

We now employ the Beck method [3] in matrix formulation. According to the formulation (1) of the IHCP, we consider zero flux boundary conditions at $x = 1$, i.e. $q_J^\nu = 0$, in the following. We assume that a single temperature transducer is located at the right end of the spatial interval, at $x = x_J = 1$.

With heat fluxes q_0^ν, $\nu = 0, \ldots, n$, at $x = 0$ and an approximation u^n for $u(., t_n)$ already computed, the Beck method determines the new heat flux q_0^{n+1} by solving the heat equation for r 'future time steps' with constant flux q_0^n at $x = 0$ and initial value u^n (for $t = t_n$)

$$C_\Delta^{(0)} \tilde{u}^{n+l} = C_\Delta^{(1)} \tilde{u}^{n+l-1} + \Delta t\, Q_0 q_0^n \qquad \tilde{u}^n = u^n \qquad l = 1, \ldots, r \tag{7}$$

where $Q_0 = Q_0^{(0)} + Q_0^{(1)}$.

In the above examples, Q_0 is nothing other than the multiplication of the fluxes in the first component by $2/h$.

Now, q_0^{n+1} is obtained by one Newton step for minimizing the defect between the computed $\tilde{u}_J^{n+l}$ and the data $g^{n+l} = g(t_{n+l})$, $l = 1, \ldots, r$ (cf 4.4.3 in [4])

$$q_0^{n+1} = q_0^n + \sum_{l=1}^{r} \gamma_l^{(r)} \left(g^{n+l} - \tilde{u}_J^{n+l}\right) \tag{8}$$

where $\gamma_l^{(r)} = s_J^l / \Delta^{(r)}$ denote the *gain coefficients*, $\Delta^{(r)} = \sum_{l=1}^{r} (s_J^l)^2$ and s_J^l are the *sensitivity coefficients* obtained by solving the heat equation with vanishing initial value and flux equal to one at $x = 0$ for $t > 0$

$$C_\Delta^{(0)} s^{\nu+1} = C_\Delta^{(1)} s^\nu + \Delta t\, Q_0 1 \qquad \nu = 0, 1, \ldots \qquad s^0 = 0. \tag{9}$$

The sensitivity coefficients are nothing other than the corresponding numerical approximations for $\partial u / \partial q$ with $q = -u_x|_{x=0}$, and represent the solution of the 'step heat flux' test case.

For non-singular $C_\Delta^{(0)}$, we can write down explicit representations of $\tilde{u}^{n+l}$ and s^l which can easily be verified by induction (cf, e.g. 11.2.(41) in [15])

$$\tilde{u}^{n+l} = C_\Delta^l u^n + q_0^n s^l \tag{10}$$

with

$$s^l = \Delta t \sum_{\mu=1}^{l} C_\Delta^{l-\mu} C_\Delta^{(0)-1} Q_0 1 \tag{11}$$

for $l = 1, \ldots, r$, where $C_\Delta = C_\Delta^{(0)-1} C_\Delta^{(1)}$.

We insert (10) into (8) and obtain for the new surface heat flux using Beck's method

$$q_0^{n+1} = \left(1 - \Delta t \sum_{l=1}^{r} \gamma_l^{(r)} \sum_{\mu=1}^{l} P_J C_\Delta^{l-\mu} C_\Delta^{(0)-1} Q_0\right) q_0^n + \sum_{l=1}^{r} \gamma_l^{(r)} \left(g^{n+l} - P_J C_\Delta^l u^n\right). \tag{12}$$

Here, P_j denotes the canonical mapping $Pj = (0, \ldots, 0, 1, 0, \ldots, 0)^{\mathrm{T}}$, $j \in \{0, \ldots, J\}$, which maps a vector to its jth component.

It is important to notice that the factor before q_0^n in (12) vanishes. Indeed, inserting (10) into (8) leads to

$$q_0^{n+1} = q_0^n + \sum_{l=1}^{r} \gamma_l^{(r)} \left[g^{n+l} - P_J(C_\Delta^l u^n + s^l q_0^n)\right]$$

$$= \left(1 - \sum_{l=1}^{r} \gamma_l^{(r)} P_J s^l\right) q_0^n + \sum_{l=1}^{r} \gamma_l^{(r)} \left[g^{n+l} - P_J C_\Delta^l u^n\right]$$

where

$$\sum_{l=1}^{r} \gamma_l^{(r)} P_J s^l = 1$$

according to the definition of the gain coefficients. Thus, only the second term in (12) appears in the representation of q_0^{n+1}. This is in accordance with formula (4.4.24) in [4] since $C_\Delta^l u^n$ is the discrete solution of the heat equation with vanishing surface heat fluxes and initial value u^n (at $t = t_n$). Considering the differential equation itself, an analogous representation of q_0^{n+1} is derived in [18] (see equation (17) and the proof of theorem 1 in [18]).

A combination of both the numerical approximation (2) of the heat equation and the sequential procedure (12) for determining the new heat flux, leads to an extended system of equations

$$C_\Delta^{(0)} u^{n+1} - \Delta t Q_0^{(0)} q_0^{n+1} = C_\Delta^{(1)} u^n + \Delta t Q_0^{(1)} q_0^n \tag{13}$$

$$q_0^{n+1} = \sum_{l=1}^{r} \gamma_l^{(r)} \left(g^{n+l} - P_J C_\Delta^l u^n\right). \tag{14}$$

This system (for calculating u^{n+1} and q_0^{n+1}) is obviously decoupled and one can first compute q_0^{n+1} from the second equation (14) and then solve the first equation (13) to obtain u^{n+1}. The second step can be viewed as calculating an update of $\tilde{u}^{n+1}$ with the new q_0^{n+1} as the flux boundary value at $x = 0$.

4. Stability analysis

We are now in a position to analyse the method of (13), (14) from the point of view of a classical stability analysis for initial value problems. This approach was also used by Cialkowski [6, 7]; our system (13), (14) can be viewed as a certain example of Cialkowski's approach with Beck's method as one suitable sequential procedure for calculating the heat fluxes at $x = 0$.

The classical stability analysis of discretization methods for initial value problems provides conditions to ensure the uniform boundedness of arbitrary powers of the matrix $C_\Delta = C_\Delta^{(0)-1} C_\Delta^{(1)}$ with respect to certain norms. For the maximum norm, positivity properties can be used to obtain the desired boundedness provided the step-size ratio $\Delta t/h^2$ lies in a certain range. With respect to the discrete L^2-norm—or to the spectral norm for the matrices—the well known von-Neumann condition provides a necessary and, in certain cases, also a sufficient condition for the boundedness of C^{ν}_{Δ}.

In this paper, we analyse both the backward Euler and Crank–Nicolson difference method and we use positivity arguments—or, in other words, maximum principles. The same approach can be applied to difference methods derived from Galerkin approximations. For the L^2-norm an approach using Fourier analysis may be carried out along the same lines.

We repeat the difference equations in (2) for solving problem (1)

$$(1+2\lambda\Theta)v_0^{k+1} - 2\lambda\Theta v_1^{k+1} = (1-2\lambda(1-\Theta))v_0^k + 2\lambda(1-\Theta)v_1^k + 2\lambda h(\Theta q + (1-\Theta)q_0^k) \tag{15}$$

$$(1+2\lambda\Theta)v_j^{k+1} - 2\Theta\left(v_{j+1}^{k+1} + v_{j-1}^{k+1}\right) = (1-2\lambda(1-\Theta))v_j^k + \lambda(1-\Theta)\left(v_{j+1}^k + v_{j-1}^k\right) \tag{16}$$

$$(1+2\lambda\Theta)v_J^{k+1} - 2\lambda\Theta v_{J-1}^{k+1} = (1-2\lambda(1-\Theta))v_J^k + 2\lambda(1-\Theta)v_{J-1}^k. \tag{17}$$

For $\Theta = \frac{1}{2}$ and $\Theta = 1$ we have the Crank–Nicolson and backward Euler method, respectively; $\lambda = \Delta t/h^2$ denotes the *mesh ratio.*

Using the representation (14) of the estimated surface heat fluxes, the *discrete Beck method* consists of the following three steps:

(a) Compute $\tilde{v}^{n+l} = C^l_{\Delta}u^n$, $l = 1, \ldots, r$, by setting $k = n, \ldots, n+r-1$, $q_0^k = q^n$ for $k = n$, $q = 0$ for $k = n+1, \ldots, n+r-1$, in (15)–(17);
(b) calculate q_0^{n+1} from (14);
(c) compute u^{n+1} from (15)–(17) by setting $k = n$ and $q = q_0^{n+1}$.

In the following, the mesh ratio is required to satisfy

$$\lambda \leqslant \frac{1}{2(1-\Theta)}. \tag{18}$$

This is the (classical) requirement for this type of difference method to be of 'positive type'; for the backward Euler method, obviously no restriction is present. Under (18), the norm of the difference operator C_{Δ} is bounded by one with respect to the maximum norm. We utilize these classical arguments to prove stability estimates for the solutions u^{n+1}, q_0^{n+1} of (13), (14).

Theorem 1. Let condition (18) be satisfied. Then, for the discrete Beck method, the estimated surface heat fluxes (see step (b)) and the approximate solutions of the IHCP at time $t = t_{n+1}$ (see (13) and step (c)), satisfy the following estimates

$$\frac{1}{S_{\Delta}^{(r)}}|q_0^{n+1}| \leqslant \max_{0\leqslant j\leqslant J}|u_j^n| + 2\lambda h|q_0^n| + \max_{1\leqslant l\leqslant r}|g^{n+l}| \tag{19}$$

$$\max_{0\leqslant j\leqslant J}|u_j^{n+1}| \leqslant \left(1+2\Theta\lambda h S_{\Delta}^{(r)}\right)\max_{0\leqslant j\leqslant J}|u_j^n| + 2\lambda h\left[(1-\Theta) + 2\Theta\lambda h S_{\Delta}^{(r)}\right]|q_0^n| + 2\Theta\lambda h S_{\Delta}^{(r)}\max_{1\leqslant l\leqslant r}|g^{n+l}| \tag{20}$$

where $S_{\Delta}^{(r)} = \sum_{l=1}^r \gamma_l^{(r)}$, and $\gamma_l^{(r)}$ are the gain coefficients which are non-negative.

Proof.
(i) By induction we show that $s_j^n \geqslant 0,\ 0 \leqslant j \leqslant J$, which also implies that $\gamma_l^{(r)} \geqslant 0$ for all l, r. For $n = 0$, this is true. Let it hold for n, then for the right-hand side of (16) (with $v_j^k = s_j^n$) we obtain by means of (18)

$$(1 - 2\lambda(1-\Theta))s_j^n + \lambda(1-\Theta)(s_{j+1}^n + s_{j-1}^n) \geqslant \min_{0\leqslant\nu\leqslant J} s_\nu^n \geqslant 0 \qquad j = 1, \dots, J-1.$$

Thus, also for the left-hand side of (18)

$$(1 + 2\lambda\Theta)s_j^{n+1} - \lambda\Theta\left(s_{j+1}^{n+1} + s_{j-1}^{n+1}\right) \geqslant 0 \qquad j = 1, \dots, J-1.$$

Writing this as $(L_h s^{n+1})_j$, the associated difference operator L_h is of negative type. Hence, $s_j^{n+1},\ j = 0, \dots, J$, assumes its non-positive minimum at $j = 0$ or $j = J$, which can also be stated as

$$\min_{0\leqslant j\leqslant J} s_j^{n+1} \geqslant \min(0, s_0^{n+1}, s_J^{n+1})$$

(cf, e.g. 8.1 in [15]). At the boundary point where a minimum appears, the first-order difference quotient is negative or the function is constant.

It should be mentioned here, that by means of the same arguments as above, the right-hand side of (15)—with $v_\nu^{k+1} = s_\nu^{n+1}$, $q = q_0^k = q_0^n = 1$, $n \geqslant 1$—is positive; the right-hand side of (17) for $v_\nu^{k+1} = s_\nu^{n+1}$ is non-negative.

Let us now assume that $s_0^{n+1} < 0$ or $s_J^{n+1} < 0$. Then a negative minimum is present, which must be assumed to be at $j = 0$ or $j = J$. If the minimum is present at $j = 0$, then $s_0^{n+1} < s_1^{n+1}$ or s_j^{n+1} is constant. The first case leads to a contradiction since the left-hand side of (15) is positive

$$s_0^{n+1} > \frac{2\lambda\Theta}{1+2\lambda\Theta} s_1^{n+1} > \frac{2\lambda\Theta}{1+2\lambda\Theta} s_0^{n+1} > s_0^{n+1}.$$

For the constant case we are led to the following contradiction

$$s_0^{n+1} > \frac{2\lambda\Theta}{1+2\lambda\Theta} s_1^{n+1} = \frac{2\lambda\Theta}{1+2\lambda\Theta} s_0^{n+1} > s_0^{n+1}.$$

If the minimum is assumed at $j = J$, the same arguments hold. Thus $s_0^{n+1} \geqslant 0$ and $s_J^{n+1} \geqslant 0$ which, together with the above estimate, proves $s_j^{n+1} \geqslant 0$ for all $j = 0, \dots, J$.

(ii) Using (18), in (15)–(17) the solution v_j^{k+1} can be estimated as

$$\max_{1\leqslant j\leqslant J-1} |v_j^{k+1}| \leqslant \frac{2\lambda\Theta}{1+2\lambda\Theta} \max_{0\leqslant j\leqslant J} |v_j^k| + \frac{1}{1+2\lambda\Theta} \max_{0\geqslant j\leqslant J} |v_j^k|$$

$$|v_0^{k+1}| \leqslant \frac{2\lambda\Theta}{1+2\lambda\Theta}|v_1^{k+1}| + \frac{1}{1+2\lambda\Theta} \max_{0\leqslant\nu\leqslant 1} |v_\nu^k| + \frac{2\lambda h}{1+2\lambda\Theta}(\Theta|q| + (1-\Theta)|q_0^k|)$$

$$|v_J^{k+1}| \leqslant \frac{2\lambda\Theta}{1+2\lambda\Theta}|v_{J-1}^{k+1}| + \frac{1}{1+2\lambda\Theta} \max_{J-1\leqslant\nu\leqslant J} |v_\nu^k|.$$

Hence, using the relation

$$\left(1 - \frac{2\lambda\Theta}{1+2\lambda\Theta}\right) = \frac{1}{1+2\lambda\Theta}$$

we obtain

$$\max_{0\leqslant j\leqslant J}|v_j^{k+1}| \leqslant \max_{0\leqslant j\leqslant J}|v_j^k| + 2\lambda h(\Theta|q| + (1-\Theta)|q_0^k|). \tag{21}$$

We therefore have the following estimate for $\tilde{v}^{n+l}$ in step (a) of the Beck method

$$\max_{0\leqslant j\leqslant J}\left|\tilde{v}_j^{n+l}\right| \leqslant \max_{0\leqslant j\leqslant J}|u_j^n| + 2\lambda h|q_0^n| \qquad l = 1,\ldots,r.$$

Using this in step (b), we obtain

$$\begin{aligned}|q_0^{n+1}| &\leqslant \sum_{l=1}^{r}\left|\gamma_l^{(r)}\tilde{v}_j^{n+l}\right| + \sum_{l=1}^{r}\left|\gamma_l^{(r)}g^{n+l}\right| \\ &\leqslant \sum_{l=1}^{r}\left|\gamma_l^{(r)}\right|\left\{\max_{0\leqslant j\leqslant J}|u_j^n| + 2\lambda h|q_0^n| + \max_{1\leqslant l\leqslant r}|g^{n+l}|\right\}\end{aligned}$$

which proves (19). Applying (21) to step (c) and using the above estimate for $|q_0^{n+1}|$ yields

$$\begin{aligned}\max_{0\leqslant j\leqslant J}|u_j^{n+1}| &\leqslant \max_{0\leqslant j\leqslant J}|u_j^n| + 2\lambda h\big(\Theta|q_0^{n+1}| + (1-\Theta)|q_0^n|\big) \\ &\leqslant \big(1 + 2\Theta\lambda h S_\Delta^{(r)}\big)\max_{0\leqslant j\leqslant J}|u_j^n| + 2\lambda h\big[(1-\Theta) + 2\Theta\lambda h S_\Delta^{(r)}\big]|q_0^n| \\ &\quad + 2\Theta\lambda h S_\Delta^{(r)}\max_{1\leqslant l\leqslant r}|g^{n+l}|.\end{aligned}$$

□

We mention here that the non-negativity of the sensitivity and gain coefficients has an analogue in a corresponding property of the solution of the step heat flux test case. The latter is zero at initial time $t = 0$; the surface heat flux is 1 for $x = 0$, $t > 0$, and vanishes at $x = 1$ for all time. The corresponding maximum principle states that this function has its minimum at $t = 0$ and thus is non-negative for all $t \geqslant 0$ (cf, e.g. chapter 8.4 in [20]).

Considering (19) and (20), stability in the classical sense would require that $\lambda h S_\Delta^{(r)} = O(\Delta t)$ which is equivalent to $S_\Delta^{(r)} = O(h)$. This cannot be achieved in the ill-posed problem under consideration, as the values of $S_\Delta^{(r)}$ in table 1 show. However, a weak instability of the form

$$\lambda h S_\Delta^{(r)} = O(1) \tag{22}$$

which is equivalent to

$$\Delta t/h \leqslant c/S_\Delta^{(r)} \tag{23}$$

would imply that the (theoretical) bounds of the sequential algorithm grow linearly with respect to the maximum norm. As in other sequential or iterative algorithms this is acceptable from the point of view of numerical analysis.

The numbers in table 1 are calculated by using the Crank–Nicolson method with an equidistant grid in the spatial interval of mesh size $h = 1/20$. The computed $S_\Delta^{(r)}$ show how they depend on the size of the time step width Δt and the number r of future times.

Table 1. $S_\Delta^{(r)}$ for various values of Δt and r.

	r							
Δt	1	2	3	4	5	6	7	8
0.0100	9.9×10^9	9.9×10^9	1.5×10^5	2.0×10^4	5.1×10^3	1.9×10^3	8.8×10^2	4.8×10^2
0.0125	9.9×10^9	2.2×10^6	2.7×10^4	4.7×10^3	1.4×10^3	6.2×10^2	3.2×10^2	1.9×10^2
0.0200	5.6×10^6	2.7×10^4	1.6×10^3	4.3×10^2	1.8×10^2	9.9×10^1	6.2×10^1	4.3×10^1
0.0250	6.8×10^5	5.5×10^3	5.4×10^2	1.8×10^2	8.5×10^1	5.0×10^1	3.4×10^1	2.4×10^1
0.0400	1.9×10^4	4.3×10^2	9.1×10^1	4.0×10^1	2.3×10^1	1.6×10^1	1.2×10^1	9.1×10^0
0.0500	4.9×10^3	1.7×10^2	4.6×10^1	2.3×10^1	1.4×10^1	1.0×10^1	7.7×10^0	6.2×10^0
0.0800	4.8×10^2	3.7×10^1	1.5×10^1	8.6×10^0	6.0×10^0	4.6×10^0	3.7×10^0	3.1×10^0
0.1000	2.0×10^2	2.1×10^1	9.4×10^0	5.9×10^0	4.2×10^0	3.3×10^0	2.7×10^0	2.3×10^0
0.2000	2.3×10^1	5.4×10^0	3.1×10^0	2.2×10^0	1.7×10^0	1.4×10^0	1.2×10^0	1.0×10^0

Increasing r or Δt (or both) leads to a decrease of $S_\Delta^{(r)}$, which makes the sequential procedure more stable in the sense of (22), (23). Thus, on the basis of our stability condition, we have regained the fact—known from computational experiments for a long time—that the Beck method becomes more stable when r or Δt are increased.

It has been also analysed how the $S_\Delta^{(r)}$ depend on the spatial mesh width h. Calculating $S_\Delta^{(r)}$ with $h = \frac{1}{20}, \frac{1}{16}, \frac{1}{10}, \frac{1}{8}$ shows a rather big difference in the first two rows and in the first column of the table where the $S_\Delta^{(r)}$ are large. Here the values for $h = \frac{1}{8}$ are up to 100% larger than those for $h = \frac{1}{20}$. In the other portions of the table the numbers depend very little on h. In every case the $S_\Delta^{(r)}$ increase when h is increased.

We now discuss another aspect of our stability conditions (23). This condition can be understood as a strengthened form of the classical Courant–Friedrichs–Lewy condition. The latter is a stability condition for numerical methods of solving hyperbolic equations. Since the surface heat fluxes are approximated by means of the Beck method, the relationship to hyperbolic problems is not astonishing. When the surface temperature itself is the control, a modified sequential method proceeds quite analogously, where, instead of flux boundary conditions at $x = 0$, one has to take Dirichlet conditions. In this case the gain coefficients and the $S_\Delta^{(r)}$ differ from the above and the corresponding stability condition reads $\lambda S_\Delta^{(r)} = O(1)$. This is then a stronger form of the classical stability condition for numerical methods of solving parabolic equations.

At the end of this section two further remarks should be made. Firstly, the analysis of the discrete version of Beck's method for multiple sensor positions (cf 4.4.3 in [4]) is straightforward and can be carried out along the same lines as above. Secondly, an extension to two-dimensional rectangular domains is possible by means of the approach developed by Reinhardt [16].

5. Numerical experiments

The final section is devoted to a presentation and discussion of computational results. The following three examples will be considered:

Example 1.

$$u(x,t) = t + \tfrac{1}{2}(1-x)^2 \qquad 0 \leqslant x \leqslant 1,\ 0 \leqslant t \leqslant 1$$

$$q(t) = 1 \qquad f(t) = t + \tfrac{1}{2} \qquad g(t) = t \qquad 0 < t \leqslant 1.$$

Example 2.

$$u(x,t) = t^2 + (1-x)^2 t + \tfrac{1}{12}(1-x)^4 \qquad 0 \leqslant x \leqslant 1,\ 0 \leqslant t \leqslant 1$$

$$q(t) = 2t + \tfrac{1}{3} \qquad f(t) = t^2 + t + \tfrac{1}{12} \qquad g(t) = t^2 \qquad 0 < t \leqslant 1.$$

Example 3. Triangular heat flux test case (cf section 5.2.3 in [4])

$$u(0,t) = \frac{1}{2}t^2 + \frac{1}{3}t - \frac{1}{45} + \frac{2}{\pi^4}\sum_{k=1}^{\infty}\frac{1}{k^4}\exp(-\pi^2 k^2 t)$$

$$u(1,t) = \frac{1}{2}t^2 - \frac{1}{6}t - \frac{7}{360} + \frac{2}{\pi^4}\sum_{k=1}^{\infty}\frac{(-1)^k}{k^4}\exp(-\pi^2 k^2 t).$$

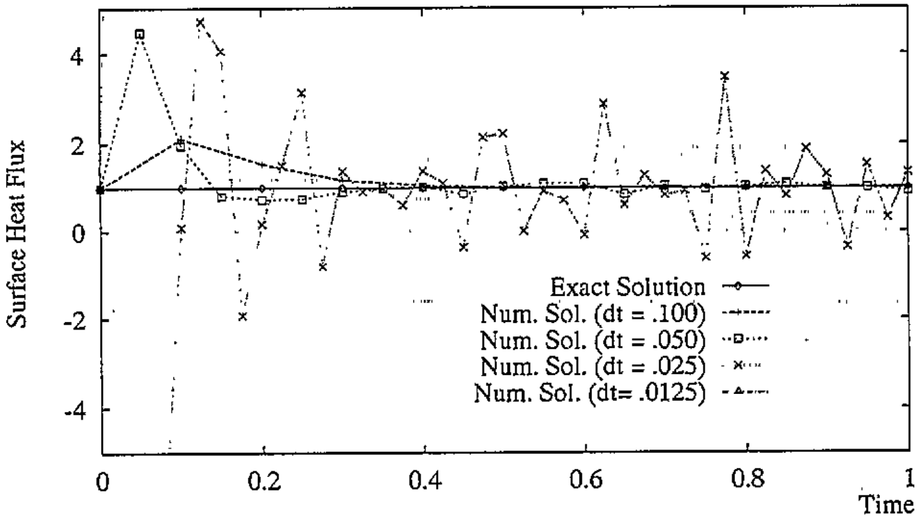

Figure 1. Surface heat flux for example 1 ($r = 4$, random perturbation, $h = \frac{1}{8}$, $\varepsilon = 5 \times 10^{-3}$).

Figure 1 shows that the constant heat flux in example 1 is stably computed with $r = 4$ future times as long as the time step size is not smaller than $\Delta t = 0.025$; the curve for $\Delta t = 0.0125$ is not seen in the figure because its values are far out of the indicated range. In figures 2 and 3 the numerical solutions of surface temperature $f(t)$ for example 1 are displayed with no perturbations in the temperature data at $x = 1$ (figure 2) and noisy data caused by random perturbations of the data of magnitude $\varepsilon = 5\times10^{-3}$ (figure 3). Obviously, $r = 6$ and $r = 8$ for $\Delta t = 0.0125$ stabilizes the computations; even with errorless data, $r = 4$ is not enough to perform stable calculations—the corresponding curve is not visible in figure 2. The spatial mesh size is chosen to be $h = \frac{1}{8}$.

For example 2, figures 4–6 display the corresponding results to figures 1–3 for example 1. The same observations as above can be made as far as the magnitude of Δt and r are concerned.

Investigating the influence of the spatial mesh size h for the selected combinations of r and Δt, figure 7 indicates an improvement of the computational results—at least for

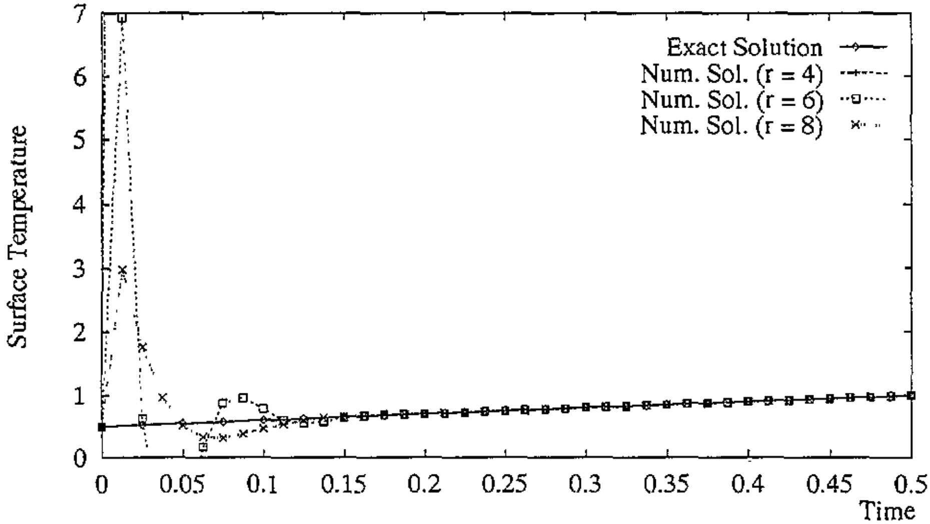

Figure 2. Surface temperature for example 1 ($dt = 0.0125$, $h = \frac{1}{8}$, $\varepsilon = 0$).

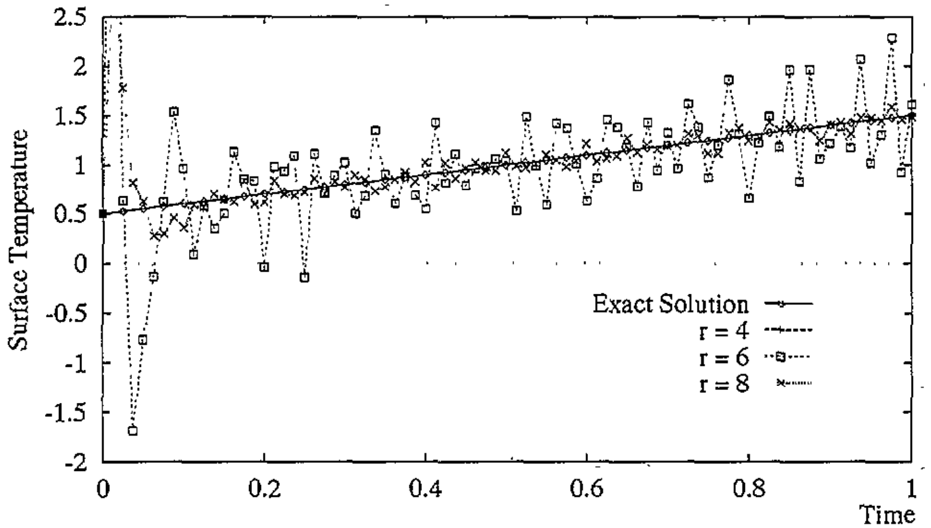

Figure 3. Surface temperature for example 1 (random perturbation, $dt = 0.0125$, $h = \frac{1}{8}$, $\varepsilon = 5 \times 10^{-3}$).

errorless data—when h is halved to $\frac{1}{16}$; the numerical solution is not accurate but it remains bounded. This is in accordance with our stability condition (23) when we take into account the observation that $S_{\Delta}^{(r)}$ decreases from 1.2×10^4 (for $h = \frac{1}{8}$) to 5.1×10^3 (for $h = \frac{1}{16}$). Note that the left-hand side of (23) is doubled which nearly compensates for the increase of the right-hand side. Nevertheless, $\Delta t, r$ and h are in a range where the described improvement is present; the same observation can be made for example 1—and also for example 3 (the corresponding figures are not shown here).

Figures 8–11 are related to the triangular heat flux test case (example 3). For $r = 4$ only

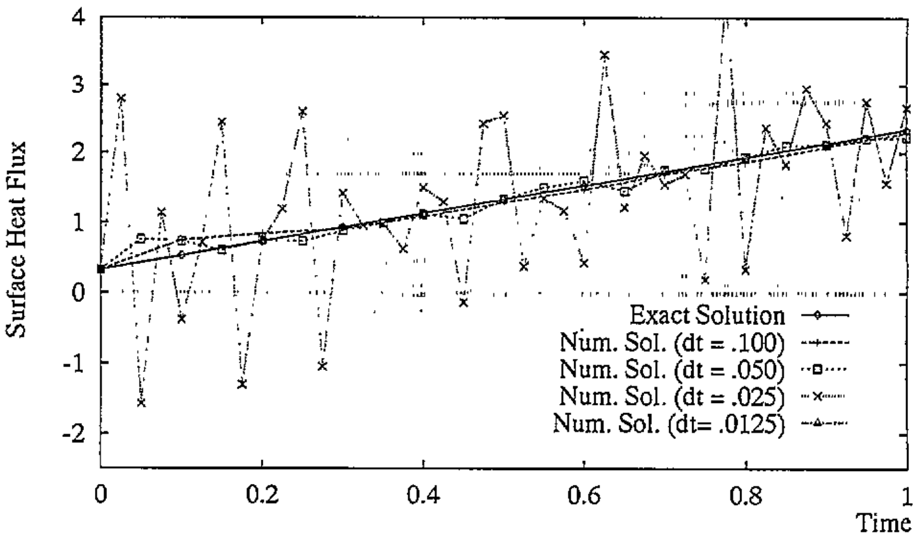

Figure 4. Surface heat flux for example 2 ($r = 4$, random perturbation, $h = \frac{1}{8}$, $\varepsilon = 5 \times 10^{-3}$).

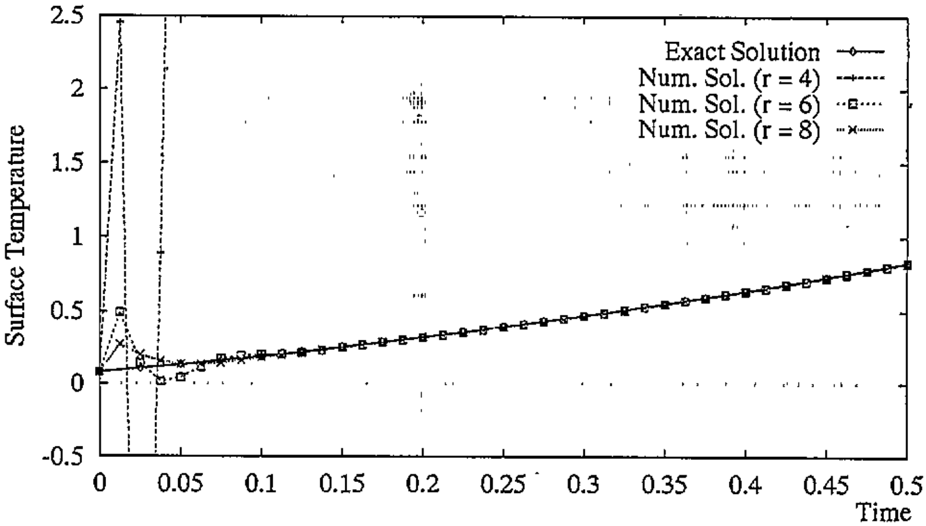

Figure 5. Surface temperature for example 2 ($dt = 0.0125$, $h = \frac{1}{8}$, $\varepsilon = 0$).

relatively large Δt provide stable computations as shown in figure 8. Even with errorless data, the same $r = 4$ and $\Delta t = 0.0125$ produce useless numerical solutions after a few time steps (see figure 9) which can be made stable by using larger r ($r = 6$ or 8). According to figure 10, the same statement can be made if data errors $\varepsilon\varphi^n$ of magnitude $\varepsilon = 5 \times 10^{-3}$ are imposed with randomly created $\varphi^n \in [-1, 1]$; again the curve for $\Delta t = 0.0125$ is not visible due to instability. Figure 8 is chosen analogously to figure 6, but with random errors of magnitude 5×10^{-3}; for $r = 6$ and 8 the errors remain bounded, while for $r = 4$ the errors explode and are not visible in the figure.

In example 3, even with errorless data, instability is present for the same combinations

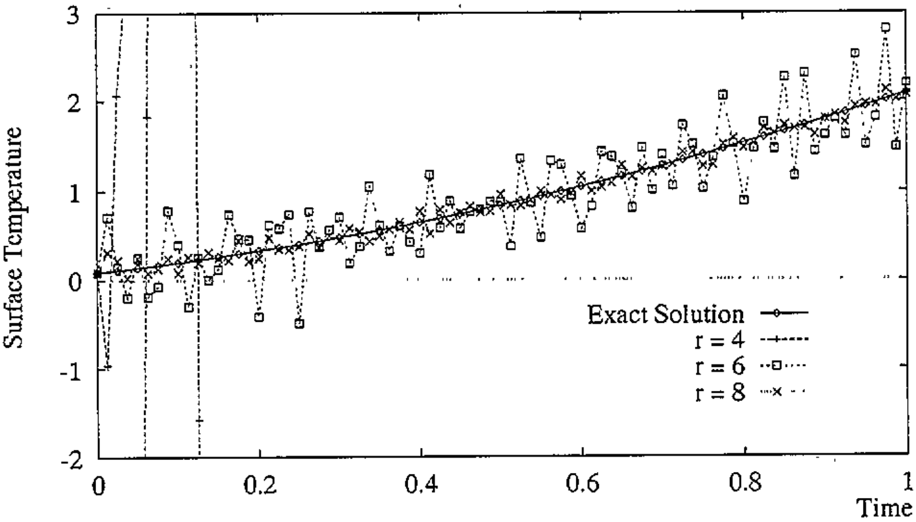

Figure 6. Surface temperature for example 2 (random perturbation, $dt = 0.0125$, $h = \frac{1}{8}$, $\varepsilon = 5 \times 10^{-3}$).

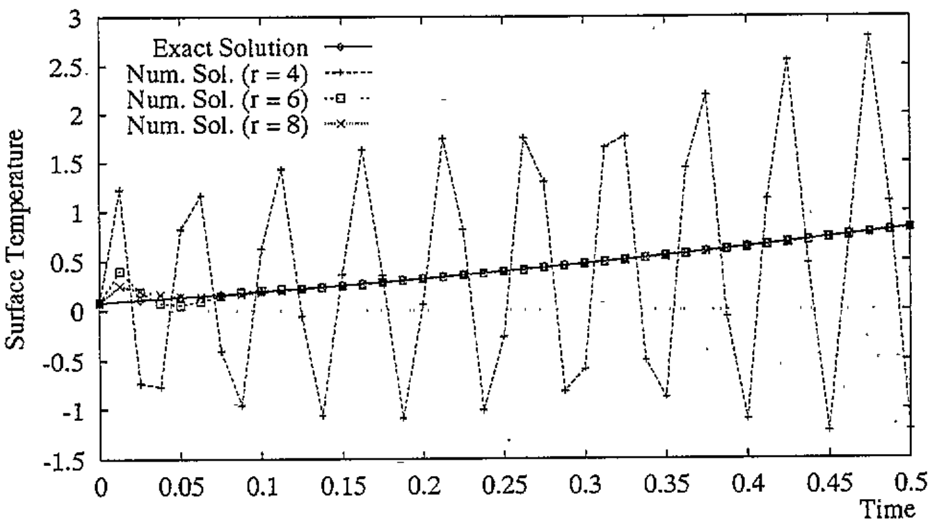

Figure 7. Surface temperature for example 2 ($dt = 0.0125$, $h = \frac{1}{16}$, $\varepsilon = 0$).

of r and Δt as for perturbed data. A possible explanation is the fact that in this example the data are always perturbed due to the cutting of the infinite series in the representation of the solution. Comparing figure 7 for example 2 with the computations including randomly created data perturbations of magnitude $\varepsilon = 5 \times 10^3$, for example, the computations are no longer stable (the corresponding curves are not displayed here). Thus, in this example, an existing data perturbation indeed makes the problem more ill posed and the computations can become unstable.

Our computations suggest a conclusion which may help to decide *a priori* what choices

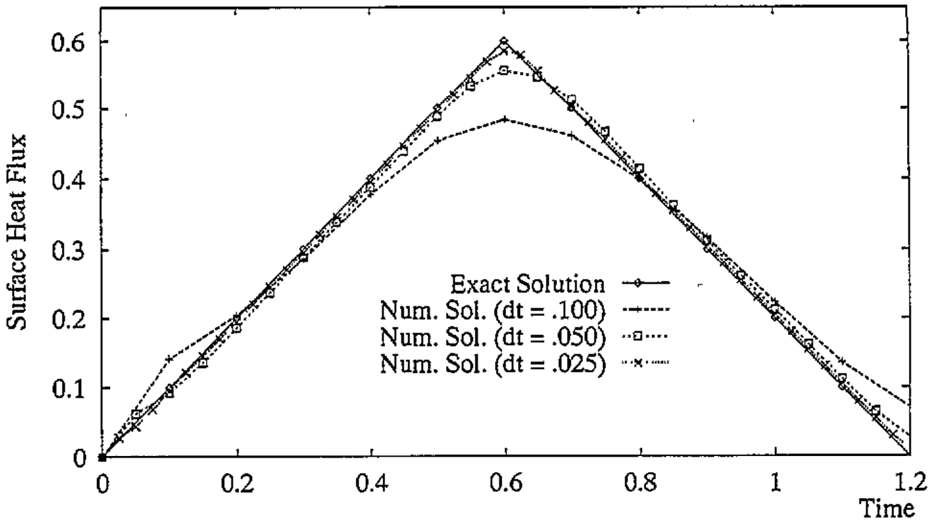

Figure 8. Triangular heat flux for example 3 ($r = 4$, $h = \frac{1}{8}$, $\varepsilon = 0$).

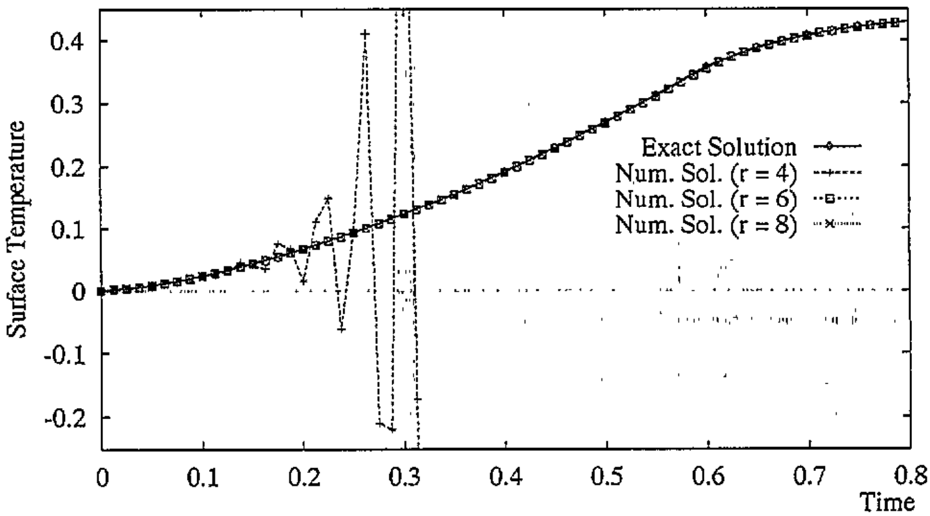

Figure 9. Triangular heat flux ($dt = 0.0125$, $h = \frac{1}{8}$, $\varepsilon = 0$).

of Δt and r lead to stable calculations. If we choose $c = 1 \times 10^3$ in (23) then, in our examples, the calculations are stable as long as (23) is satisfied—otherwise the computations are unstable. However, we think that more examples and test calculations are needed to decide how c in (23) has to be chosen.

References

[1] Baumeister J and Reinhardt H-J 1987 On the approximate solution of a two-dimensional inverse heat

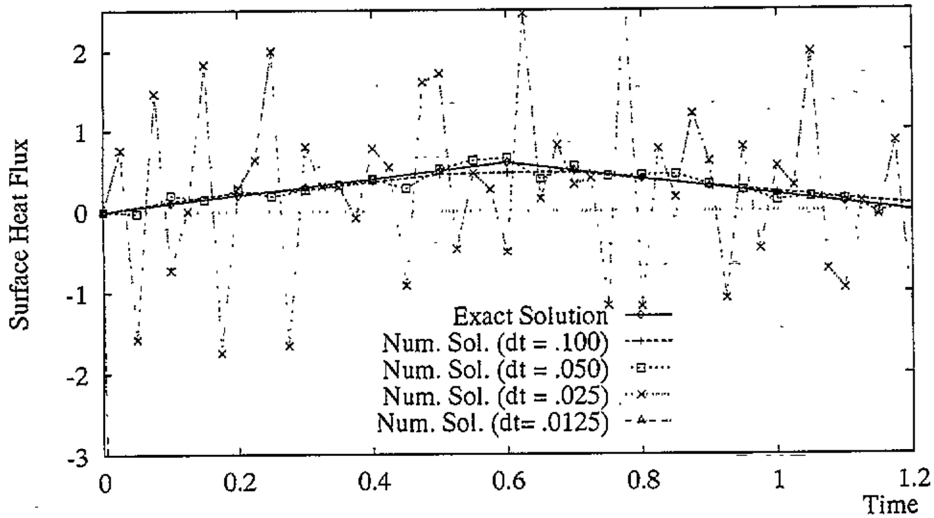

Figure 10. Triangular heat flux ($r = 4$, random perturbation, $h = \frac{1}{8}$, $\varepsilon = 5 \times 10^{-3}$).

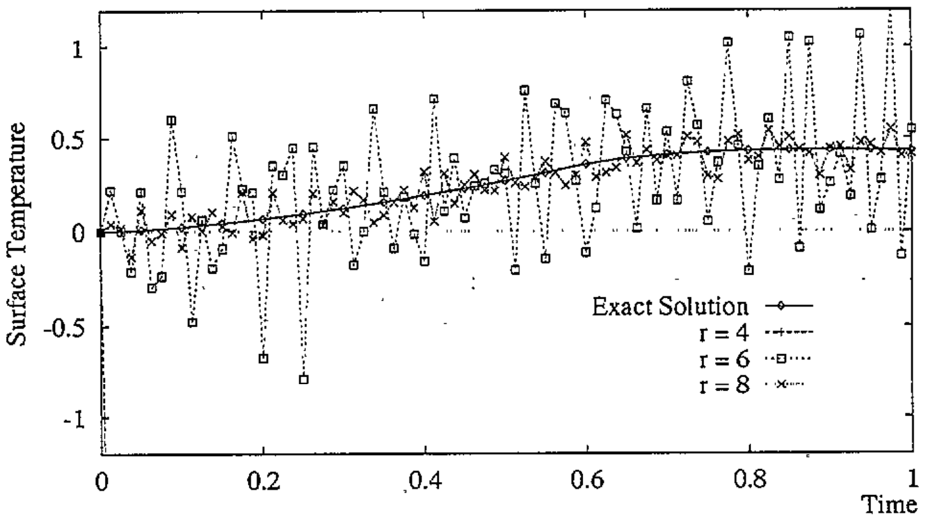

Figure 11. Triangular heat flux (random perturbation, $dt = 0.0125$, $h = \frac{1}{8}$, $\varepsilon = 5 \times 10^{-3}$).

conduction problem *Inverse and Ill-posed Problems (St Wolfgang, 1986)* ed H W Engl and C W Groetsch (Boston: Academic) pp 325–44

[2] Beck J V 1970 Nonlinear estimation applied to the nonlinear inverse heat conduction problem *Int. J. Heat Mass Transfer* **13** 703–16

[3] Beck J V, Litkouhi B and St Clair C R Jr 1982 Efficient sequential solution of the nonlinear inverse heat conduction problem *Num. Heat Transfer* **5** 275–86

[4] Beck J V, Blackwell B and St Clair C R Jr 1985 Inverse Heat Conduction Problems (New York: Wiley)

[5] Carasso A 1982 Determining surface temperatures from interior observations *SIAM J. Appl. Math.* **42** 558–74

[6] Cialkowski M J, Grysa K and Jankowski J 1992 Inverse problem of linear non-stationary heat transfer equation *Z. Angew. Math. Mech.* **72** T611–4

[7] Cialkowski M 1993 Numerische Lösung des inversen Problems für eine nichtlineare und nichtstationäre Wärmegleichung *Z. Angew. Math. Mech.* 73 T684–9

[8] Dinh Nho Hào A mollification method for ill-posed problems *Numer. Math.* in press

[9] Dinh Nho Hào and Gorenflo R 1991 A non-characteristic Cauchy problem for the heat equation *Acta Appl. Math.* 24 1–27

[10] Dinh Nho Hào 1992 A non-characteristic Cauchy problem for linear parabolic equations. II: A variational method *Numer. Funct. Anal. Optim.* 13 541–64

[11] Knabner P and Vessella S 1987 Stabilization of ill-posed Cauchy problems for parabolic equations *Ann. Mat. Pura Appl.* 149 393–409

[12] Knabner P and Vessella S 1987 Stability estimates for ill-posed Cauchy problems for parabolic equations *Inverse and Ill-Posed Problems (St Wolfgang, 1986)* ed H W Engl and C W Groetsch (Boston: Academic) pp 351–68

[13] Knabner P and Vessella S 1988 The optimal stability estimate for some ill-posed Cauchy problems for a parabolic equation *Math. Methods Appl. Sci.* 10 575–83

[14] Levine H A 1983 Continuous data dependence, regularization and a three lines theorem for the heat equation with data in a space like direction *Ann. Mat. Pura Appl.* 134 267–87

[15] Reinhardt H-J 1985 *Analysis of Approximation Methods for Differential and Integral Equations (Applied Mathematical Sciences, vol 57)* (New York: Springer)

[16] Reinhardt H-J 1991 A numerical method for the solution of two-dimensional inverse heat conduction problems *Int. J. Numer. Methods Eng.* 32 363–83

[17] Reinhardt H-J 1993 On the stability of sequential methods solving the inverse heat conduction problem *Z. Angew. Math. Mech.* 73 T928–30

[18] Reinhardt H-J 1993 Analysis of sequential methods solving the inverse heat conduction problem *Num. Heat Transfer* B 24 455–74

[19] Seidman T I and Eldén L 1990 An 'optimal filtering' method for the sideways heat equation *Inverse Problems* 6 681–96

[20] Zauderer E 1983 *Partial Differential Equations of Applied Mathematics* (New York: Wiley)